Increased Collagen I/ Collagen III Ratio Is Associated with Hemorrhage in Brain Arteriovenous Malformations in Human and Mouse

Zahra Shabani , Joana Schurger , Xiaonan Zhu , Chaoliang Tang , Li Ma , Alka Yadav , Rich Liang , Kelly Press , Shantel Weinsheimer , Annika Schmidt , Calvin Wang , Abinav Sekhar , Helen Kim , hua su *

Posted Date: 6 December 2023

doi: 10.20944/preprints202312.0389.v1

Keywords: Brain arteriovenous malformation; Collagen I; Collagen III; Microhemorrhage; Depletion of microglia; Gluycoprotein nonmetastatic B

Research paper

Increased Collagen I/Collagen III Ratio Is Associated with Hemorrhage in Brain Arteriovenous Malformations in Human and Mouse

Zahra Shabani [1,2], Joana Schurger [1,2], Xiaonan Zhu [1,2], Chaoliang Tang [1,2], Li Ma [1,2], Alka Yadav [1,2], Rich Liang [1,2], Kelly Press [1,2], Shantel Weinsheimer [1,2], Annika Schmidt [1,2], Calvin Wang [1,2], Abinav Sekhar [1,2], Helen Kim [1,2] and Hua Su [1,2,*]

[1] Center for Cerebrovascular Research, University of California, San Francisco, San Francisco, CA, United States.
[2] Department of Anesthesia and Perioperative Care, University of California, San Francisco, San Francisco, CA, United States.
* Correspondence: Hua Su, Department of Anesthesia and Perioperative Care; University of California, San Francisco, 2540 23rd Street, Box 1363, San Francisco, CA 94143; Phone: 415-476-0141, Email: hua.su@ucsf.edu, ORCID: 0000-0003-1566-9877

Abstract: Background: Increase of collagen I (COL I)/COL III ratio enhances vessel wall stiffness and renders vessels less resistant to blood flow and pressure changes. We hypothesized that COL I/COL III ratio is increased in the brain arteriovenous malformations (bAVMs), which is associated with bAVM hemorrhage. **Method:** Surgically resected human bAVM samples and mouse bAVMs induced in three transgenic mouse lines with activin receptor-like kinase 1 or endoglin deletion in the endothelial cells or in the brain focally. Colony-stimulating factor receptor inhibitor was used to transiently deplete microglia. COL I and COL III levels, hemorrhage, and gene expression in bAVMs were analyzed. **Results:** The COL I and COL III levels and the COL I/COL III ratio were higher on human and mouse bAVMs than controls, which was associated with bAVM hemorrhage. Col I and Col III mRNAs were also increased in mouse bAVMs. The degree of microhemorrhage in mouse bAVMs was positively correlated with Col I/Col III ratios. Transient depletion of microglia reduced Col I/Col III ratio and microhemorrhage in mouse bAVMs. **Conclusion:** COL I/COL III ratio are increased in bAVM vessels, which is associated with bAVM hemorrhage. Depletion of microglia reduces Col I/Col III ratio and hemorrhage in mice bAVMs.

Keywords: brain arteriovenous malformation; Collagen I; Collagen III; microhemorrhage; depletion of microglia; gluycoprotein nonmetastatic B

Introduction

Intracerebral hemorrhage (ICH) constitutes around 10 – 15% of stroke and causes high early mortality in patients [1]. Brain arteriovenous malformations (bAVMs) are one of the most frequent sources of non-traumatic ICH. About 50% of bAVM cases present initially with ICH [1,2]. Brain AVM is a tangle of dysplastic vessels that shunts blood from the arteries to veins. There are no capillary in bAVM nidus [3]. The progression of bAVMs to ICH remains incompletely understood.

The extracellular matrix (ECM) is a main constituent of the cellular microenvironment and generates an intricate three-dimensional network [4]. The vascular ECM consists primarily the basement membrane and the interstitial ECM. The interstitial ECM is composed of elastic fibers and fibrillar collagens and is located in the media surrounding the vascular smooth muscle cells (SMCs) of the large vessel walls, which maintains normal vessel wall stiffness and elasticity to mechanically control shear stress and pressure [5].

Elastin and collagens are major ECM elements in the arteries. Seventeen collagen types have been recognized in the mouse aorta. Collagen I (COL I) and COL III are the most abundant collagens in the vascular wall, regulating vascular homeostasis and remodeling [6]. Col I and III fibers are connected, entangled, and packed to make a firm structure [7]. Collagen I provides resistance to

 doi:10.20944/preprints202312.0389.v1

stretch, whereas COL III forms an elastic network that offers resilience and structural maintenance of the vessel wall. Several studies emphasize the contribution of the collagen system to the pathophysiology of sporadic bAVM [8,9]. Single cell RNA sequence (RNAseq) data showed that perivascular fibroblasts and fibromyocytes, the major cells that produce COLs, are strongly associated with the development of sporadic bAVMs in humans, and are found in proximity to the peri-lesional macrophages [10]. In addition, the contents of COL I and COL III in ruptured AVMs were higher than that of non-ruptured AVMs [7]. Nevertheless, the mechanisms underlying these changes have not been studied.

It has been shown that microglia accumulation is associated with fibroblast proliferation. Gluycoprotein nonmetastatic B $(GPNMB)^+$ monocytes have been identified in human bAVMs [10], which may contribute to collagen synthesis in part through activating fibroblasts [3,11,12]. Further, it has been shown that the crosstalk of platelets with macrophages and fibroblasts aggravates inflammation and aortic wall stiffening [13]. Thus, microglia and monocytes may play roles in activation of fibroblasts in bAVMs. In this study, we examined COL I/COL III ratio in surgically resected bAVM tissues and bAVMs in mice models and the association of COL I/COL III ratio with bAVM hemorrhage. We also tested if depletion of microglia reduces the Col I/Col III ratio and bAVM hemorrhage.

2. Materials and Methods

2.1. Ethics statement

Human brain tissues and clinical data were obtained from the University of California San Francisco (UCSF) with protocols approved by the Institutional Review Board and Ethics Committee (IRB: 10-02012). All tissues were acquired from patients undergoing neurosurgical operations and written informed consent was obtained before the procedure permitting collection of tissue specimens for research. For nonvascular lesion controls, temporal lobe specimens were similarly acquired from subjects undergoing anterior temporal lobectomy for medically refractory epilepsy.

All animal experimental protocols were approved by the Institutional Animal Care and Use Committee (IACUC) of the UCSF. The staff of the IACUC of UCSF Animal Core Facility provided animal husbandry according to the guidance of certified Animal Technologists. Veterinary care was offered by IACUC faculty members and veterinary inhabitants located on the San Francisco General Hospital campus. All mice were maintained in a pathogen free area in 421×316 cm2 cages and were kept on a 12-h light and dark cycle with free access to food and water.

2.2. Human Specimens

Diagnoses of human bAVMs were confirmed by preoperative angiography, and fresh tissues were acquired as part of planned surgical resection. All specimens were fresh frozen in OCT and sectioned into 20-mm-thick sections using a Leica RM2155 microtome (Leica Microsystems, Wetzlar, Germany).

2.3. Animals

We used 8- to 10-week-old mice in this study. Both male and female mice were used. For induction of bAVMs in mice, the following genetically modified mouse lines were used: 1) *Pdgfb*icreER;*Eng*$^{f/f}$.; 2) *Pdgfb*icreER;*Alk1*$^{f/f}$ and 3) *Alk1*$^{f/f}$. The *Pdgfb*icreER;*Eng*$^{f/f}$ and *Pdgfb*icreER;*Alk1*$^{f/f}$ have platelet-derived growth factor (pdgf) promoter driven estrogen inducible cre recombinase expression in the endothelial cells (ECs) and have endoglin (*Eng*) gene exons 5-6 floxed [14] or activin receptor line kinase 1 (*Alk1, also known as Acvrl1*) gene exons 4-6 floxed [15]. *Alk1*$^{f/f}$ mice have *Alk1* gene exons 4-6 floxed [15].

Preprints (www.preprints.org) | NOT PEER-REVIEWED | Posted: 6 December 2023 doi:10.20944/preprints202312.0389.v1

2.4. Brain AVM model induction and viral vector delivery in mice

Brain AVMs were induced in *Pdgfb*icreER;*Alk1*$^{f/f}$ mice through intra-brain injection of an adeno-associated viral vector expressing vascular endothelial growth factor [AAV-VEGF, 2×10^9 genome copies (vgs)] to induce brain focal angiogenesis and intra-peritoneal (i.p.) injection of tamoxifen (TM, 1.25 mg/kg of body weight) 14 days later to delete *Alk1* gene in ECs (Figure 1A) [16,17]. Brain AVMs in *Pdgfb*icreER;*Eng*$^{f/f}$ mice were induced through intra-brain injection of AAV-VEGF (2×10^9 vgs) and i.p. injection of TM (2.5 mg/kg) for three consecutive days starting on the day of intra-brain injection of AAV-VEGF to delete *Eng* gene in ECs (Figure 1B) [18]. Control *Pdgfb*icreER;*Alk1*$^{f/f}$ mice and *Pdgfb*icreER;*Eng*$^{f/f}$ mice received intra-brain injection of AAV-VEGF and i.p. corn oil injection. Brain AVM in *Alk1*$^{f/f}$ was induced by co-injection of an adenoviral vector expressing Cre recombinase (Ad-Cre; 2 × 10^7 plaque-forming units) to delete the *Alk1* gene in the brain focally and AAV-VEGF (2×10^9 vgs) to induce brain angiogenesis (Figure 1C) [19]. Control mice for *Alk1*$^{f/f}$ model received intra-brain injection of Ad-GFP and AAV-VEGF. Brain samples were collected 8 weeks after model injection for analyses (Figure 1).

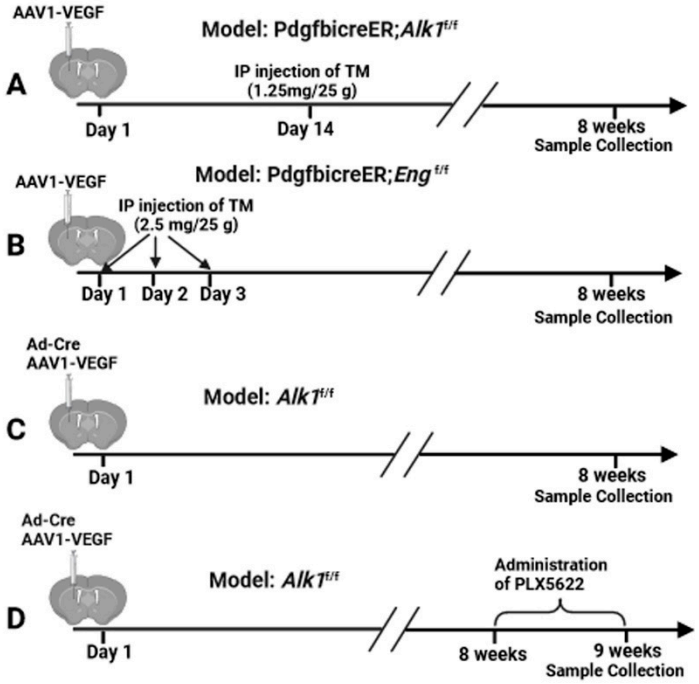

Figure 1. Study design. A, B & C. Induction of bAVM in *Pdgfb*icreER;*Alk1*$^{f/f}$, *Pdgfb*icreER;*Eng*$^{f/f}$, and *Alk1*$^{f/f}$ mice. **(D)** PLX5622 treatment.

For injection of viral vectors into mouse brain, mice were anesthetized with 4% isoflurane inhalation and were placed in a stereotactic apparatus with a mouth holder (David Kopf Instruments, Tujunga, CA, USA). A burr hole was drilled in the pericranium 2 mm lateral and 1 mm posterior to the bregma. A 10 µl Hamilton syringe was inserted into the right basal ganglia 3 mm beneath the brain surface. Two microliters of viral suspension were slowly injected at a rate of 0.2 µl per minute. The needle was withdrawn after 10 minutes, and the wound was closed with a 4-0 suture.

2.5. Administration of CSF1R inhibitor (PLX5622)

PLX5622 (180 mg/kg of body weight/day, Plexikon Biotech Company, South San Francisco, CA) was incorporated in chow and orally administered for 7 days starting at 8 weeks after bAVM model induction in *Alk1*$^{f/f}$ mice. The placebo chow was administrated in the same manner to the control group (Figure 1D).

 doi:10.20944/preprints202312.0389.v1

2.6. Immunofluorescence staining of human and mouse sections

For human samples, two sections of each bAVM and control brain tissues were co-stained with antibodies specific to human COL I and CD31 or COL III and CD31 using rabbit anti-COL I (1:250, NBP1-30054, Novus Bio-Tecne, Centennial, CO), goat anti Col III (1:250, 1330-01, Southern Biotec, Birmingham, AL) and mouse anti-CD31 (1:100, 14-0319-82, eBioscience, San Diego, CA). Sections were incubated with primary antibodies at 4°C overnight. After washing with PBS, donkey anti-mouse antibody conjugated with Alex Flour 594 (Thermo Fisher Scientific, Cat#A21203, 1:200), donkey anti-goat antibody conjugated with Alexa Fluor 488 (Thermo Fisher Scientific, Cat#A1105, 1:300), and donkey anti-rabbit antibody conjugated with Alexa Fluor 488 (Thermo Fisher Scientific, Cat#A32790, 1:300) were used as secondary antibody to visualize positive stains. Vectashield anti-fade mounting medium containing 4',6-diamidino-2-phenylindole (DAPI) (Vector Laboratories, Cat# H-1200, Burlingame, CA) was used to stain the cell nuclei and mount the slide. Sections were examined and imaged using a Keyence fluorescence microscopy under a 20x objective lens (Model BZ-9000, Keyence Corporation of America, Itasca, IL). A total of 10 images were taken from each brain sample, five from each section for analyses.

To study mouse samples, the mice were anesthetized with 4% isoflurane inhalation, and their brains were collected, frozen in dry ice and cut into 20-mm-thick coronal sections with a Leica RM2155 Microtome (Leica Microsystems). Two sections per brain adjacent to injection site were selected and co-stained with Col I and CD31 or Col III and CD31 using mouse anti-Col I (1:250, NB600-450, Novus Biotechne), goat anti-Col III (1:250, 1330-01, Southern Biotech) and rat anti-CD31 (1:100, SC-18916, Santa Cruz, CA) antibodies. For Col I stain, sections were blocked for 1 hour in the M.O.M. kit blocker (one drop/5ml, MKB-2213-1, Vector Laboratory, Newark, CA). After incubating at 4°C overnight with primary antibodies, sections were washed with PBS and were incubated with donkey anti-rat antibody conjugated with Alexa Fluor 488 (Thermo Fisher Scientific, Cat # A-21208, 1:100), donkey anti-mouse antibody conjugated with Alexa Fluor 594 (1:300), and donkey anti-goat antibody conjugated with Alexa Fluor 594 (Thermo Fisher Scientific, Cat #A-11058, 1:300) for 1.5 hours at room temperature. $CD68^+$ and $GPNMG^+$ cells were stained on two sections per mouse brain adjacent to the injection site with a rat anti mouse CD68 antibody (1:250 MCA1957, Bio-Rad, Hercules, CA), and rabbit anti-GPNMB (AB188222, 1:200 abcam, Cambridge, UK) as described above. The sections were then incubated with donkey anti-rabbit antibody conjugated with Alexa Fluor 488 (Thermo Fisher Scientific, Cat #A-21206, 1:400) for 1.5 hours at room temperature. After incubated with the secondary antibodies, all sections were mounted with Vectashield anti-fade mounting medium DAPI (Vector Laboratories, Cat# H-1200). Mouse brain sections were examined and imaged using a Keyence fluorescence microscopy under a 20X objective lens (Model BZ-9000, Keyence Corporation of America). A total of six images were taken from each brain samples, three from each brain section (to the right, to the left and below the injection site).

The images were coded by a researcher who did not participate in the quantification. All quantifications were performed by at least two researchers who were blinded to the group assignment. COL I, COL III and CD31 stained areas were quantified using NIH image J 1.63 software. The number of $CD68^+$ cells and $GPNMB^+$ cells were counted manually.

2.7. Prussian Blue Staining

Two sections per brain adjacent to the injection site were used for detecting iron deposition using an Iron Stain Kit (Sigma-Aldrich, St. Louis, MO). Slides were incubated in a freshly prepared working iron stain solution for 15 min, washed in distilled water, and then counterstained with pararosaniline solution for 3 min. Data are presented as Prussian blue-positive area/mm^2.

2.8. RNA-Seq analysis

Total RNA was isolated from bAVM lesions and brain angiogenic regions (controls) and sent to Novogene Co (Davis, CA) for sequencing using the company's standard protocol (**Supplemental Material 1**). The outcome data were also analyzed by Novogen Co.

 doi:10.20944/preprints202312.0389.v1

2.9. Statistical analysis

For quantification of COL I and COL III levels, $CD68^+$ cells, $GPNMB^+$ cells and Prussian blue positive areas, section numbers were scrambled. The quantification was done independently by at least two researchers who were blinded to the treatment groups. A histogram was used to test if the data were normally distributed. Data were represented as mean ± SD. The differences between the two groups were analyzed by two sample *t*-tests. One-way ANOVA was used for multiple sample comparisons followed by Tukey's multiple comparisons using GraphPad Prism Version 9 software. A p-value < 0.05 was considered to be significant. We applied a log transformation (Log Y) to the Col I and Col III levels before performing analysis because the data were not normally distributed. Sample sizes were indicated in the figures.

3. Results

3.1. Human ruptured bAVMs have higher COL I and COL III levels and COL I/ COL III ratio than unruptured bAVMs

We found that the levels of COL I and COL III were increased in both rupture (2.49±0.12 for COL I, 2.22±0.12 for COL III, *ps*<0.001) and unruptured (2.43±0.06 for COL I, 2.26±0.06 for COL III, *ps*<0.001) sporadic bAVMs compared to the controls (1.87±0.03 for COL I, 1.79±0.06 for COL III, Figure 2, A-F). The COL I/ COL III ratio was higher in ruptured bAVM compared to unruptured bAVM (1.90±0.27 for ruptured bAVMs vs. 1.46±0.15 for unruptured bAVMs, p= 0.005; Figure 2, G). These data revealed that increase of the levels of COL I and COL III as well as COL I/ COL III ratio are associated with bAVM rupture.

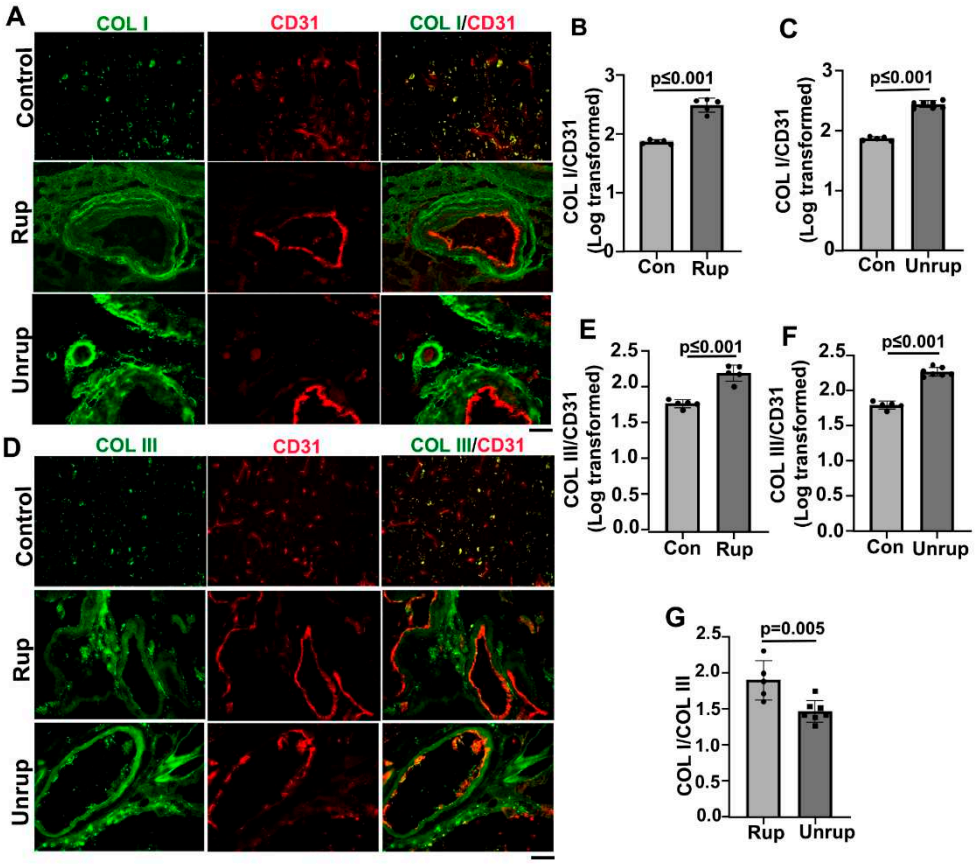

Figure 2. COL I and COL III levels and COL I/ COL III ratio are higher in ruptured than unruptured bAVMs. A & D. Representative images of COL I (green) and COL III (green) antibody-stained sections. ECs (red) were stained by an anti-CD31 antibody. Scale bar= 50 μm. **B, C, E, & F.** Quantifications of COL I and COL III levels on vessels. **G**. Quantification of COL I/COL III ratio. Con:

Preprints (www.preprints.org) | NOT PEER-REVIEWED | Posted: 6 December 2023 doi:10.20944/preprints202312.0389.v1

controls; Rup: ruptured bAVMs; Unrup**:** unruptured bAVMs. N=6 for control, N=5 for ruptured bAVMs, and N=7 for unruptured bAVMs.

COL I and COL III levels in human HHT bAVM were also higher than controls (COL I: $p<0.001$, and COL III: $p<0.001$, Supplementary Figure S1, A, B, D). In addition, HHT AVMs displayed higher COL I/COL III ratio than controls ($p=0.034$). Our results indicate that COL I and COL III levels as well as the COL I/COL III ratio are also increased in HHT bAVMs.

3.2. Mouse bAVMs have higher Col I/Col III ratio which are associated with microhemorrhage

We found that bAVMs in *Pdgfb*icreER;*Alk1*$^{f/f}$ and *Pdgfb*icreER;*Eng*$^{f/f}$ mice exhibited higher levels of Col I and Col III compared to brain angiogenic regions in controls. In *Pdgfb*icreER;*Alk1*$^{f/f}$ mice, the Col I levels in bAVMs are 1.88±0.11, while in the brain angiogenic region of corn oil treated mice are 1.22±0.09 ($p<0.001$). The Col III in bAVMs of *Pdgfb*icreER;*Alk1*$^{f/f}$ mice are 1.72±0.20; in brain angiogenic region of corn oil-treated mice are 1.35±0.14 ($p=0.002$). The Col I/Col III ratio in *Pdgfb*icreER;*Alk1*$^{f/f}$ bAVMs (1.72±0.20) is also higher than that in brain angiogenic region of corn oil-treated mice (1.35±0.34, p=0.006, Figure 3A, B, D, E & G).

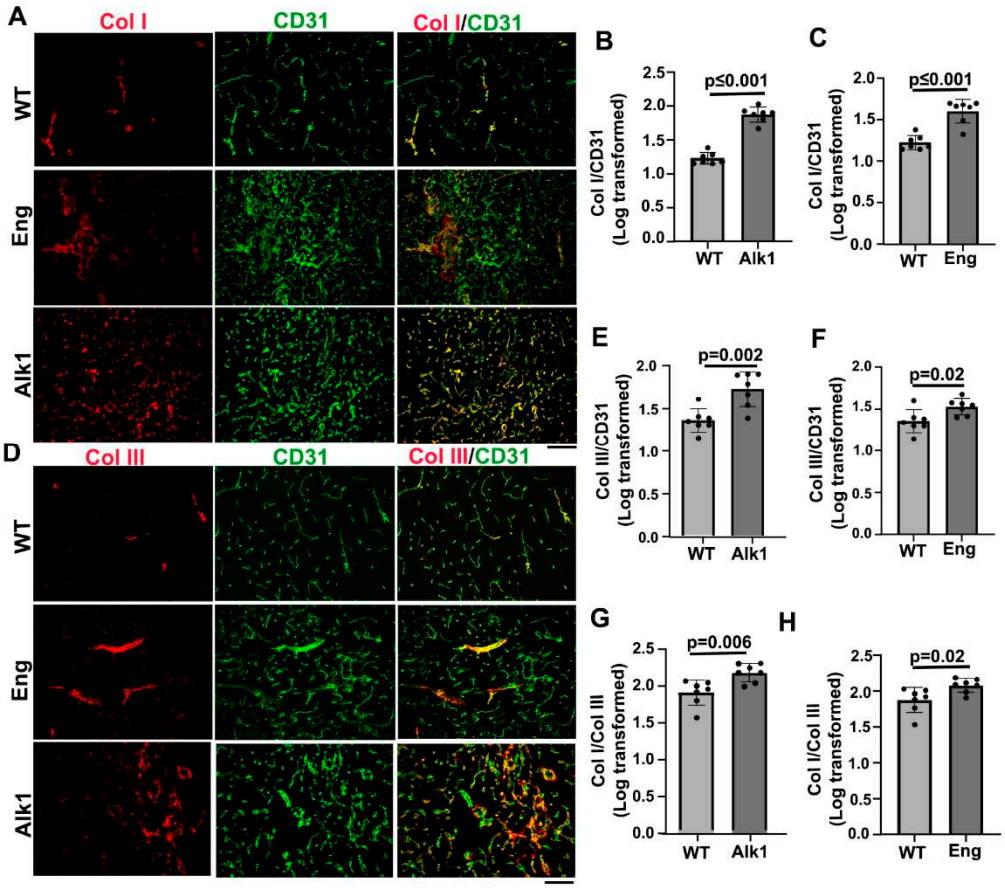

Figure 3. Col I, Col III and Col I/Col III ratio are higher in mouse bAVMs than the brain angiogenic region of control mice. A & D. Representative images of Col I (red) and Col III (red) antibody stained sections. ECs (green) were stained by an anti-CD31 antibody. Scale bar=50 μm. B & E. Quantifications of COL I and COL III levels in bAVMs in *Pdgfb*icreER;*Alk1*$^{f/f}$ mice. G. Quantification of COL I/COL III ratios in bAVMs in *Pdgfb*icreER;*Alk1*$^{f/f}$ mice. C & F. Quantifications of COL I and COL III levels in bAVMs in *Pdgfb*icreER;*Eng*$^{f/f}$ mice. H. Quantification of Col I/Col III ratios in bAVM in *Pdgfb*icreER;*Eng*$^{f/f}$ mice. WT: corn oil-treated controls; Alk1: *Pdgfb*icreER;*Alk1*$^{f/f}$ mice; Eng: *Pdgfb*icreER;*Eng*$^{f/f}$ mice. N=7.

In *Pdgfb*icreER;*Eng*$^{f/f}$ mice, the Col I levels in bAVMs are 1..60±0.14, while in the brain angiogenic region of corn oil-treated mice are 1.22±0.09 ($p<0.001$). The Col III levels in bAVMs of

Preprints (www.preprints.org) | NOT PEER-REVIEWED | Posted: 6 December 2023 doi:10.20944/preprints202312.0389.v1

*Pdgfb*icreER;*Eng*$^{f/f}$ mice are 1.53±0.10; in brain angiogenic region of corn oil treated mice are 1.35±0.14 (p=0.02). The Col I/Col III ratio in the *Pdgfb*icreER;*Eng*$^{f/f}$ bAVMs (2.08±0.10) is also higher than brain angiogenic region of corn oil-treated mice (1.87±0.17, p=0.02, Figure 3A, C, D & H).

Microhemorrhages in the bAVMs and control brain angiogenic regions were analyzed by Prussian blue staining. We found more iron depositions in bAVMs of *Pdgfb*icreER;*Alk1*$^{f/f}$ (p=0.015) and *Pdgfb*icreER;*Eng*$^{f/f}$ (p=0.016) compared to brain angiogenic regions of corn oil treated mice (Figure 4) indicating the presence of microhemorrhage in bAVMs. The Prussian blue–positive areas were positively correlated with the Col I/Col III ratio (p= 0.007, r=0.52, r^2=0.27, Figure 4D). Collectively, these data suggest that a higher Col I/Col III ratio is associated with greater microhemorrhage in mouse bAVMs.

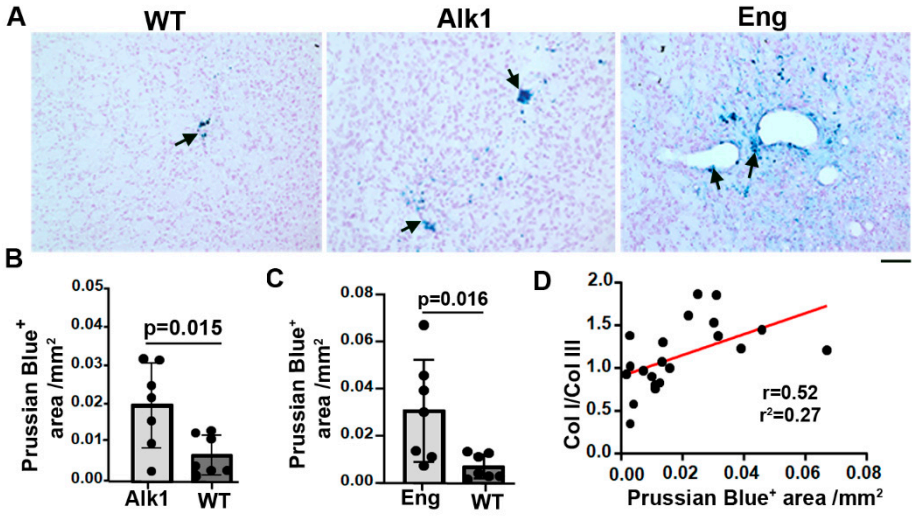

Figure 4. Microhemorrhage in mouse bAVMs. A. Representative images of Prussian blue stained sections. Iron positive areas are stained blue (arrows). Scale bar=50 μm. **B & C.** Quantification of Prussian blue positive areas. WT**:** corn oil-treated controls; Alk1: *Pdgfb*icreER;*Alk1*$^{f/f}$ mice; Eng**:** *Pdgfb*icreER;*Eng*$^{f/f}$ mice. N=7. **D.** Correlations of Prussian blue positive areas and Col I/Col III ratios.

3.3. Transient depletion of Central nervous system (CNS) macrophages/microglia reduced Col I/Col III ratios and microhemorrhage in bAVM

To test if reduction of inflammation by transient depletion of CNS macrophages/microglia influences Col I and Col III levels, and Col I/Col III ratios in bAVMs, *Alk1*$^{f/f}$ mice were treated with PLX5622 8 weeks after bAVM model induction for 7 days. We found that PLX5622 treatment reduced CD68$^+$ cells in bAVMs (p=0.048 versus controls, Figure 6 A & B) and Col I level (p=0.003 verses controls). PLX5622 treatment did not affect the Col III levels (p=0.33, Figure 5 A, B, C & D). The Col I/Col III ratios (p= 0.04) and microhemorrhage in PLX-treated bAVMs were lower than controls (p<0/001, Figures 5E and 6E,F). These data revealed that transient depletion of CNS macrophages/microglia decreases Col I/Col III ratio and microhemorrhage in bAVMs.

Preprints (www.preprints.org) | NOT PEER-REVIEWED | Posted: 6 December 2023 doi:10.20944/preprints202312.0389.v1

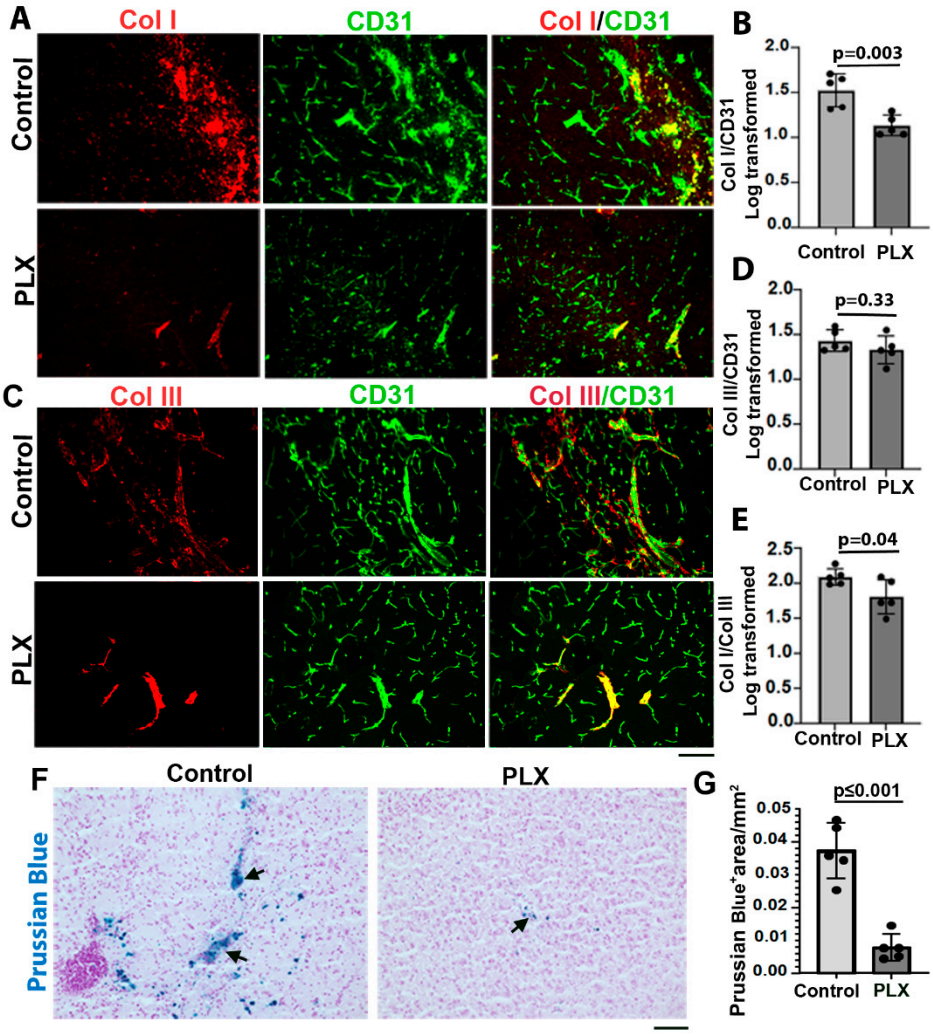

Figure 5. Transient depletion of CNS macrophage microglia reduced **Col I/Col III ratios and microhemorrhage** in bAVMs. **A & C.** Representative images of Col I (red) and Col III (red) antibody-stained sections. ECs (green) were stained by an anti-CD31 antibody. Scale bar=50 μm. **B & D.** Quantifications of COL I and COL III levels in bAVMs of PLX5622 (PLX) treated mice and placebo chow treated mice (Control). **E.** Quantification of Col I/Col III ratios in bAVMs of PLX5622 (PLX) treated mice and placebo chow treated mice (Control). N=5. **F.** Representative images of Prussian blue stained sections. Arrows: positive staining. Scale bar=50 μm. **G.** Quantification of Prussian blue positive areas. N=5.

Preprints (www.preprints.org) | NOT PEER-REVIEWED | Posted: 6 December 2023 doi:10.20944/preprints202312.0389.v1

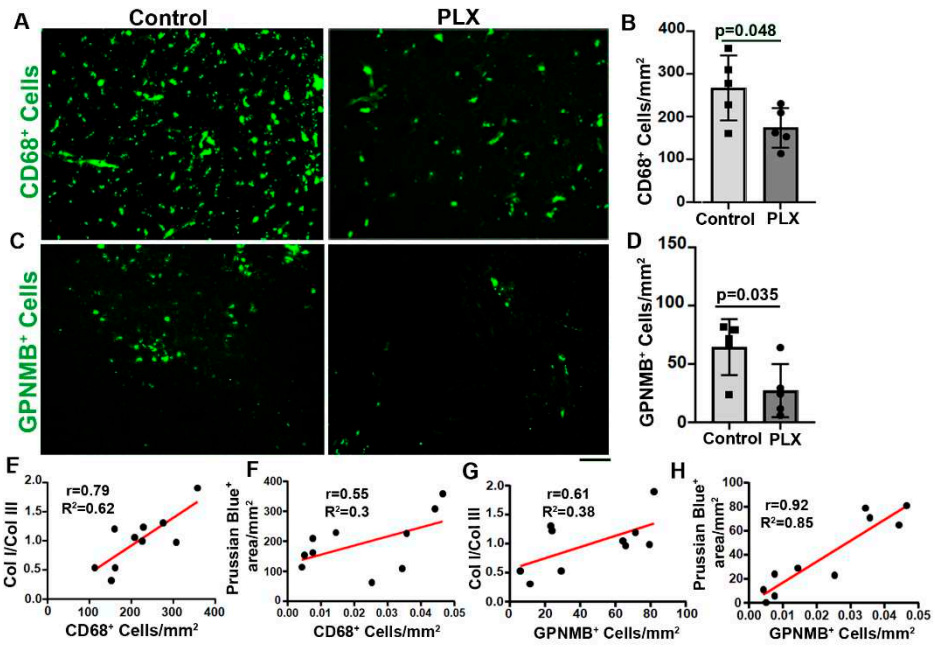

Figure 6. PLX5622 treatment reduced CD68⁺ cells and GPNMB⁺ cells in bAVMs. A-C. Representative images of sections stained with antibodies specific to CD68 (**A**) or GPNMB (**C**). Scale bar =50 μm. **B & D**. Quantification of CD68⁺ cells (**B**) and GPNMB⁺ cells (**D**). N=5. **E & F**. Correlations of CD68⁺ cells with Col I/Col III ratio (**E**) and Prussian blue⁺ areas (**F**). **G & H.** Correlations of GPNMB⁺ cells with Col I/Col III ratio (**G**) and Prussian blue⁺ areas (**H**). **PLX:** PLX5622 treated mice; Control: placebo chow treated mice.

Since it has been shown that GPNMB⁺ macrophages may contribute to collagen synthesis in part through activating fibroblasts [3,11,12], we analyzed if PLX5622 treatment affects GPNMB⁺ macrophages. We found that PLX5622 treatment not only reduced CD68+ microglia/macrophages (p=0.048, Figure 6 A & B), but also reduced the number of GPNMB⁺ macrophages in bAVMs (p= 0.042, Figure 6, C & D). The numbers of CD68⁺ and GPNMB⁺ are positively corrected with Col I/Col III ratio and microhemorrhages in bAVMs (Figure 6. G, H , I & J). Collectively, these data suggest that reduction of CD68⁺ and GPNMB⁺ cells reduce Col I/Col III ratios and microhemorrhages in bAVMs.

3.4. Fibroblast and inflammatory-related genes are upregulated in mouse bAVMs

The differential gene expression in bAVMs in *Pdgfb*icreER;*Eng*$^{f/f}$ mice and the brain angiogenic regions of control mice was analyzed through RNAseq. We identified 2143 genes that were upregulated and 1830 genes that were downregulated in bAVMs compared to controls. In addition to up-regulation of angiogenesis (*padj*=2.07E-17), vasculogenesis (*padj*=9.6E-05), acute inflammatory response (*padj*=0.042) signaling, collagen binding signaling was upregulated (*padj*=0.0001) in bAVMs analyzed by Gene Ontology (GO) enrichment analyses. Differentially analysis showed up-regulation of Col1a1 (*padj*=0.035) and Col3a1 (*padj*=0.032) gene expression in bAVMs compared to controls. Several inflammatory-related genes were also upregulated in the bAVMs, such as CD68 (*padj*=0.004), Icam2 (*padj*=0.0003) and Csf1 (*padj*=0.002). In addition, the expression of fibroblast genes, Vim (*padj*=0.019), CD34 (*padj*=0.02), CD248 (*padj*=1.8E-05), Csf2rb (*padj*=0.049), Mpeg1 (*padj*=1.7E-05) were increased in the bAVMs (Table 1). Interestingly, Timp2, (*padj*=0.01) and Timp3 (*padj*=0.04) expression were also increased in bAVMs (Table 1), which could reduce collagen degradation mediated by MMPs.

 doi:10.20944/preprints202312.0389.v1

Table 1. Upregulated pathways and expression of genes related to angiogenesis, inflammation, and collagen stability in *Eng* deficient mouse bAVMs.

Pathway name	**Adj. *p*-value**
Angiogenesis	2.07E-17
Vasculogenesis	9.6E-05
Collagen binding signaling	0.0001
Acute inflammatory response	0.042
Gene name	**Adj. *p*-value**
CD248*	1.8E-05
Mpeg1**	1.7E-05
Icam2**	0.0003
CD68**	0.004
Csf1**	0.002
Timp2	0.01
Vim*	0.019
CD34*	0.02
Col1a1***	0.035
Col3a1***	0.032
Csf2rb**	0.049
Timp2****	0.01
Timp3****	0.04

Notes: 1. Go analysis was used to evaluate pathways changes and differential analysis was used to assess differential gene expression. 2. * Fibroblast specific genes. 3. **Inflammatory related genes. 4.***a chains of Col I and Col III. 5-**** Genes related to collagen degradation.

4. Discussion

In this study, we demonstrated that COL I and COL III levels as well as the ratio of COL I/COL III are increased in human and mouse bAVMs. The ruptured sporadic bAVMs have higher levels of COL I and COL III and COL I/COL III ratios compared to unruptured bAVMs. Results obtained from mouse bAVM models are consistent with those obtained from human specimens. In mice, Col I/Col III ratio is positively correlated with the degree of bAVM hemorrhage. Furthermore, our data illustrated a positive correlation between increased Col I/Col III ratio and the degree of microhemorrhage in mouse bAVM models. In addition, transient depletion of CNS macrophages/microglia reduced Col I/Col III ratios and microhemorrhage in mouse bAVMs.

It has been reported in a study with 43 patients that severe ECs damage, fewer SMCs in the media, and hyperplasic COL I and COL III content are present in the ruptured bAVMs [7]. Guo et al. reported that collagen fibers in the internal elastic lamina of blood vessels in the human bAVM nidus are disorganized and interrupted. They also noticed an increase in COL I and a decrease in COL III levels in human bAVMs compared with control brain samples [2]. Our results are consistent with these findings.

COL I and COL III are interstitial or fibrous collagen types, which are connected together, entangled, and packed to generate a steady structure [20], wrapping the blood vessels to form an almost continuous layer [21]. COL I provides strength and resistance to stretch and deformation of vessels, while, Col III presents elasticity and resilience [22]. COL III fibers are thinner and more elastic, which afford less tensile strength than COL I, thus providing more resilience, tissue distensibility, and structural support [23]. The combination and organization of these collagen subtypes maintain the function, integrity, and strength of blood vessels. An increase of the COL I/COL III ratio in bAVM may reprensent impairment of the ECM, leading to structural instability of the vasculature in bAVM and vessel wall weakness [24].

The balance of Col I/ Col III ratio is maintained by multiple mechanisms. The levels of COL I and COL III depend not only on the production, but also on the degradation [20]. Hence, higher COL I / COL III ratio in bAVMs could be caused by overproduction of COL I or faster degradation of COL

 doi:10.20944/preprints202312.0389.v1

III. It has been shown that activation of vascular TGF-β1 and its downstream signaling effector SMAD increases the synthesis of ECM proteins such as COL I in fibroblasts. TGF-β also reduces collagenase production and inhibits COL degradation [25,26]. The fibroblast cells are predominant resident cells in the adventitial layer and are responsible for depositing abundant collagen fibrils around vessels. In addition, it has been suggested that pericytes can express Col Ia1 and Col IIIa1 [26,27]. Our RNA-seq data showed that the expression of Col1a1 and Col IIIa1 are increased in bAVM suggesting that Col I and Col III productions are increased in bAVMs.

On the other hand, endopeptidases such as matrix metallopeptidase (MMPs) can degrade ECM components, including collagens. Increased MMP activity can reduce vessel wall stability and integrity and blood-brain barrier integrity and thus increases the risk of hemorrhage [28,29]. MMP-1 is synthesized by fibroblasts and shows equal effect for COL I and COL III degradation, while MMP-8, synthesized by neutrophils, has a higher affinity for COL III. The MMP activities can be inhibited by tissue inhibitors of metalloproteinases-1 (TIMP-1) to TIMP-4 [30,31]. Therefore, the altered activities of MMPs and TIMPs may contribute to the changes in COL I and COL III ratios in bAVM [32,33]. Indeed, we found through RNAseq that the expression of Timp2 and 3 are increased in bAVMs of *Pdgfb*icre;ER;*Eng*$^{f/f}$ mice which could be one of the mechanisms responsible for the increase of Col I and Col III levels in bAVMs.

We showed that transient depletion of microglia/macrophages by PLX5622 treatment reduced Col I/Col III ratio, microhemorrhage, CD68$^+$ and GPNMB$^+$ cells in bAVMs of *Alk1*$^{f/f}$ mice. The Col I/Col III ratio and the degree of microhemorrhage are positively correlated with CD68$^+$ and GPNMB$^+$, suggesting that inflammation plays a role in the increased Col I/Col III ration in bAVMs. Microglia, the primary resident immune cells of the CNS, are key elements of neuroinflammation. Enhanced accumulation of microglia has been observed in bAVMs in both human and mouse models [34–36]. A handful of studies have indicated the association of microglia and collagen levels change [2,37]. However, the correlation between microglia/macrophages with Col I / Col III ratios and hemorrhage are poorly explored before.

GPNMB is an endogenous type 1 transmembrane glycoprotein [38]. In the CNS, GPNMB is expressed in monocytes, where it plays an important role in the regulation of inflammatory responses [39]. Winkler et al revealed that interaction between vascular and immune cells, such as GPNMB$^+$ monocytes, which can induce pathological changes associated with brain hemorrhage; they showed that GPNMB$^+$ monocytes contribute to SMCs depletion and are associated with bAVM rupture and brain hemorrhage [10]. It has been reported that GPNMB may activate resident normal fibroblasts [3]. Thus, microglia and monocytes may play roles in the activation of fibroblasts in bAVMs, resulting in increased collagen production and bAVM hemorrhage.

Our RNA-seq results showed that *Cd68*, *Csf1, and* csf1r *were upregulated in mouse bAVMs.* Csf-1 is a cytokine required for the differentiation of monocyte lineage cells. It has been shown that csf1r expression was induced during macrophage differentiation in mice. Moreover, Gpnmb RNA levels are regulated by Csf-1 during the process of macrophage differentiation [40]. According to these results, it is quite likely that Gpnmb$^+$ cells and activated macrophages are associated with changes in Col I and Col III levels via activation of residing fibroblasts and increased production of collagen fibers.

In addition to COL I and III, COL IV has also been implicated in bAVM pathogenesis. In capillary malformation-AVM with Ephrin type-B receptor 4 (*Ephb4*) or Ras p21 protein activator 1 (*Rasa1*) mutation, Col IV accumulated in the EC endoplasmic reticulum leading to EC apoptotic death [41,42]. Age-dependent increase of COL4A2 has also been reported in bAVM suggesting a potential role of COL4A2 in bAVM pathophysiology [43]. We will analyze COL IV and its relationship with COL I and III, COL IV and inflammatory cells in future.

5. Conclusion

Our results show that increased COL I /COL III ratio is associated with an increase in microhemorrhage and bAVM rupture probably via increased activated macrophages/macroglia and GPNMB$^+$ cells. Inhibition of inflammation through transient depletion of CNS

 doi:10.20944/preprints202312.0389.v1

macrophages/microglia reduces Col I /Col III ratios and microhemorrhage in mouse bAVMs. Therefore, inhibition of inflammation can be a target for the development of therapies to reduce bAVM hemorrhage.

Author Contributions: Conceptualization, Z.S., H. S,; methodology, Z.S., J.S., X. Z., C. T., L. M., H.K, A.Y., S.W, R.L. and K.P; software, Z.S.; validation, Z.S., A.S. ; formal analysis, Z.S., investigation, Z.S. J.S., H.K, A.Y., S.W, R.L. and K.P; resources, Z.S, A.S., C.W. and, A.S. ; data curation, Z.S, A.S., C.W. and, A.S; writing—original draft preparation, Z.S. and H.S.; writing—review and editing, Z.S. and H.S.; visualization, Z.S. and H.S.; supervision, H.S.; project administration, H.S.; funding acquisition, H.S. All authors have read and agreed to the published version of the manuscript.

Funding: This research was funded by the National Institutes of Health (R01 HL122774, NS027713 and NS112819) and from the Michael Ryan Zodda Foundation to H.S.

Institutional Review Board Statement: The study was conducted in accordance with the of the University of California, San Francisco (UCSF), and approved by the institutional review board and ethics committee (IRB: 10-02012, 09/30/2023). for studies involving humans. The animal study protocol was approved by the institutional Animal Care and Use Committee (IACUC) of the University of California, San Francisco (UCSF), and approved by the institutional review board and ethics committee (IACUC: AN189299-02E, 10/02/2023 and AN201883-00, 09/22,2023).

Informed Consent Statement: Written informed consent was obtained from all patients to use their de-identified data and samples for research.

Acknowledgments: We thank Dr. Mervy Maze for critically reading the manuscript.

Conflicts of Interest: The authors declare no conflict of interest.

References

1. Klebe, D., et al., *Intracerebral hemorrhage in mice.* Traumatic and Ischemic Injury: Methods and Protocols, 2018: p. 83-91.
2. Yi, G., et al., *Human brain arteriovenous malformations are associated with interruptions in elastic fibers and changes in collagen content.* Turkish Neurosurgery, 2013. **23**(1).
3. Zhang, S., et al., *CT Angiography Radiomics Combining Traditional Risk Factors to Predict Brain Arteriovenous Malformation Rupture: a Machine Learning, Multicenter Study.* Translational Stroke Research, 2023: p. 1-11.
4. Shabani, Z., et al., *Modulatory properties of extracellular matrix glycosaminoglycans and proteoglycans on neural stem cells behavior: Highlights on regenerative potential and bioactivity.* International Journal of Biological Macromolecules, 2021. **171**: p. 366-381.
5. Marchand, M., et al. *Extracellular matrix scaffolding in angiogenesis and capillary homeostasis*. in *Seminars in cell & developmental biology*. 2019. Elsevier.
6. Ma, Z., et al., *Extracellular matrix dynamics in vascular remodeling.* American Journal of Physiology-Cell Physiology, 2020. **319**(3): p. C481-C499.
7. Niu, H., et al., *Relationships between hemorrhage, angioarchitectural factors and collagen of arteriovenous malformations.* Neuroscience bulletin, 2012. **28**: p. 595-605.
8. Neyazi, B., et al., *Brain arteriovenous malformations: implications of CEACAM1-positive inflammatory cells and sex on hemorrhage.* Neurosurgical review, 2017. **40**: p. 129-134.
9. Mohr, J., et al., *Medical management with or without interventional therapy for unruptured brain arteriovenous malformations (ARUBA): a multicentre, non-blinded, randomised trial.* The Lancet, 2014. **383**(9917): p. 614-621.
10. Winkler, E.A., et al., *A single-cell atlas of the normal and malformed human brain vasculature.* Science, 2022. **375**(6584): p. eabi7377.
11. Lin, Z.-Q., et al., *Essential involvement of IL-6 in the skin wound-healing process as evidenced by delayed wound healing in IL-6-deficient mice.* Journal of Leucocyte Biology, 2003. **73**(6): p. 713-721.
12. Tanzadehpanah, H., M.H.S. Modaghegh, and H. Mahaki, *Key biomarkers in cerebral arteriovenous malformations: Updated review.* The Journal of Gene Medicine: p. e3559.
13. Wagenhäuser, M., et al., *Crosstalk of platelets with macrophages and fibroblasts aggravates inflammation, aortic wall stiffening and osteopontin release in abdominal aortic aneurysm.* Cardiovascular Research, 2023: p. cvad168.
14. Allinson, K.R., et al., *Generation of a floxed allele of the mouse Endoglin gene.* Genesis, 2007. **45**(6): p. 391-395.

15. Seo, M.C., et al., *Discoidin domain receptor 1 mediates collagen-induced inflammatory activation of microglia in culture.* Journal of neuroscience research, 2008. **86**(5): p. 1087-1095.
16. Chen, G., et al., *A large, single-center, real-world study of clinicopathological characteristics and treatment in advanced ALK-positive non-small-cell lung cancer.* Cancer medicine, 2017. **6**(5): p. 953-961.
17. Shaligram, S., et al., *Abstract TMP5: Bone Marrow-derived And Clonally Expanded Alk1-Endothelial Cells Contribute To Brain Arteriovenous Malformation In Mice.* Stroke, 2022. **53**(Suppl_1): p. ATMP5-ATMP5.
18. Choi, E.-J., et al., *Novel brain arteriovenous malformation mouse models for type 1 hereditary hemorrhagic telangiectasia.* PloS one, 2014. **9**(2): p. e88511.
19. Walker, E.J., et al., *Arteriovenous malformation in the adult mouse brain resembling the human disease.* Annals of neurology, 2011. **69**(6): p. 954-962.
20. Singh, D., V. Rai, and D.K. Agrawal, *Regulation of Collagen I and Collagen III in Tissue Injury and Regeneration.* Cardiology and cardiovascular medicine, 2023. **7**(1): p. 5.
21. Senk, A. and V. Djonov, *Collagen fibers provide guidance cues for capillary regrowth during regenerative angiogenesis in zebrafish.* Scientific reports, 2021. **11**(1): p. 19520.
22. Zannad, F., P. Rossignol, and W. Iraqi, *Extracellular matrix fibrotic markers in heart failure.* Heart failure reviews, 2010. **15**: p. 319-329.
23. Wittig, C. and R. Szulcek, *Extracellular matrix protein ratios in the human heart and vessels: how to distinguish pathological from physiological changes?* Frontiers in Physiology, 2021. **12**: p. 708656.
24. Balasubramanian, P., et al., *Collagen in human tissues: structure, function, and biomedical implications from a tissue engineering perspective.* Polymer Composites–Polyolefin Fractionation–Polymeric Peptidomimetics–Collagens, 2013: p. 173-206.
25. Harvey, A., et al., *Vascular fibrosis in aging and hypertension: molecular mechanisms and clinical implications.* Canadian Journal of Cardiology, 2016. **32**(5): p. 659-668.
26. Fujiwara, K., et al., *In situ hybridization reveals that type I and III collagens are produced by pericytes in the anterior pituitary gland of rats.* Cell and tissue research, 2010. **342**(3): p. 491-495.
27. Kuwabara, J.T. and M.D. Tallquist, *Tracking adventitial fibroblast contribution to disease: a review of current methods to identify resident fibroblasts.* Arteriosclerosis, thrombosis, and vascular biology, 2017. **37**(9): p. 1598-1607.
28. Mortensen, J.H., et al., *Fragments of citrullinated and MMP-degraded vimentin and MMP-degraded type III collagen are novel serological biomarkers to differentiate Crohn's disease from ulcerative colitis.* Journal of Crohn's and Colitis, 2015. **9**(10): p. 863-872.
29. Leeming, D.J., et al., *A novel marker for assessment of liver matrix remodeling: an enzyme-linked immunosorbent assay (ELISA) detecting a MMP generated type I collagen neo-epitope (C1M).* Biomarkers, 2011. **16**(7): p. 616-628.
30. Azevedo Martins, J.M., et al., *Tumoral and stromal expression of MMP-2, MMP-9, MMP-14, TIMP-1, TIMP-2, and VEGF-A in cervical cancer patient survival: a competing risk analysis.* Bmc Cancer, 2020. **20**(1): p. 1-11.
31. El Hajj, E.C., et al., *Extracellular Matrix in Cardiovascular Pathophysiology: Inhibitor of lysyl oxidase improves cardiac function and the collagen/MMP profile in response to volume overload.* American Journal of Physiology-Heart and Circulatory Physiology, 2018. **315**(3): p. H463.
32. Overall, C., J. Wrana, and J. Sodek, *Transcriptional and post-transcriptional regulation of 72-kDa gelatinase/type IV collagenase by transforming growth factor-beta 1 in human fibroblasts. Comparisons with collagenase and tissue inhibitor of matrix metalloproteinase gene expression.* Journal of Biological Chemistry, 1991. **266**(21): p. 14064-14071.
33. Woessner Jr, J.F., *Matrix metalloproteinases and their inhibitors in connective tissue remodeling.* The FASEB Journal, 1991. **5**(8): p. 2145-2154.
34. Park, E.S., et al., *Soluble endoglin stimulates inflammatory and angiogenic responses in microglia that are associated with endothelial dysfunction.* International Journal of Molecular Sciences, 2022. **23**(3): p. 1225.
35. Bendok, B. and I.A. Awad, *Evidence of inflammatory cell involvement in brain arteriovenous malformations: Commentary.* Neurosurgery, 2008. **62**(6).
36. Germans, M.R., et al., *Molecular signature of brain arteriovenous malformation hemorrhage: a systematic review.* World neurosurgery, 2022. **157**: p. 143-151.
37. Zhang, R., et al., *Persistent Infiltration of Active Microglia in Brain Arteriovenous Malformation Causes Unresolved Inflammation and Lesion Progression.* Stroke, 2015. **46**(suppl_1): p. A191-A191.
38. Saade, M., et al., *The role of GPNMB in inflammation.* Frontiers in immunology, 2021. **12**: p. 674739.

 doi:10.20944/preprints202312.0389.v1

39. Nakano, Y., et al., *Glycoprotein nonmetastatic melanoma protein B (GPNMB) as a novel neuroprotective factor in cerebral ischemia–reperfusion injury.* Neuroscience, 2014. **277**: p. 123-131.
40. Ripoll, V.M., et al., *Gpnmb is induced in macrophages by IFN-γ and lipopolysaccharide and acts as a feedback regulator of proinflammatory responses.* The Journal of Immunology, 2007. **178**(10): p. 6557-6566.
41. Chen, D., et al., *Angiogenesis depends upon EPHB4-mediated export of collagen IV from vascular endothelial cells.* JCI insight, 2022. **7**(4).
42. Chen, D., et al., *RASA1-dependent cellular export of collagen IV controls blood and lymphatic vascular development.* The Journal of Clinical Investigation, 2019. **129**(9): p. 3545-3561.
43. Neyazi, B., et al., *Age-dependent changes of collagen alpha-2 (IV) expression in the extracellular matrix of brain arteriovenous malformations.* Clinical Neurology and Neurosurgery, 2020. **189**: p. 105589.